J. Fluid Mech. (2006), *vol.* 552, *pp.* 127–136. © 2006 Cambridge University Press
doi:10.1017/S0022112006008627 Printed in the United Kingdom

Convective instability in wake intermediate asymptotics

By M. BELAN[1] AND D. TORDELLA[2]

[1]Dipartimento di Ingegneria Aeronautica e Spaziale, Politecnico di Milano, Via La Masa 34, 20156 Milano, Italy

[2]Dipartimento di Ingegneria Aeronautica e Spaziale, Politecnico di Torino, Corso Duca degli Abruzzi 24, 10129 Torino, Italy

(Received 3 June 2005 and in revised form 19 December 2005)

The paper presents a multiscale analysis of the intermediate region of the two-dimensional convectively unstable wake past a bluff body. A recent asymptotic expansion solution was used as basic flow (Tordella & Belan, *Phys. Fluids*, vol. 15, 2003, 1897). This solution was obtained by matching an inner to an outer flow, both of which are Navier–Stokes solutions. By introducing a spatio-temporal multiscaling into the instability problem, an inhomogeneous Orr–Sommerfeld equation and an associated modulation equation are obtained. The streamwise variation of the instability characteristics can then be deduced from the wave modulation, by considering the system to be perturbed by waves with a complex wavenumber that corresponds of the dominant saddle point of the local dispersion relation, taken at different positions downstream of the wake, and at different Reynolds numbers. The corrections of no parallelism are remarkable in the intermediate wake. When the disturbance is related to an early intermediate station, the corrections lead to absolute instability in the upstream portion of the intermediate wake, where, in addition, the spatial growth rate decreases. When the disturbance is related to a section in the far field, conditions of minimal temporal stability are reached about 20 body scales downstream. In the far field the temporal damping increases with the Reynolds number.

1. Introduction

A wake is a spatially developing flow where self-sustained oscillations arise (see e.g. Zebib 1987; Triantafyllou, Kupfer & Bers 1987). The disturbances grow first linearly and two-dimensionally in a region of absolute instability that exists downstream of the back stagnation point or trailing edge of the body which generates the wake, preceded and followed by convectively unstable regions (Mattingly & Criminale 1972; Monkewitz 1988; Yang & Zebib 1989; Hanneman & Oertel 1989; Pier 2002).

The present work focuses on the convectively unstable region of the wake that exists downstream of the absolutely unstable region namely the intermediate region of the wake that precedes the far field. We consider the linear spatially growing instability waves obtained by applying the WKBJ approximation to a spatio-temporal multiscaling treatment of the Orr–Sommerfeld instability equations. The multiscaling is carried out to account for the non-parallel effects (Bouthier 1972). In particular, we are interested in the effects associated with the lateral momentum dynamics and the Reynolds number, which are features which must be represented by the basic flow.

https://doi.org/10.1017/S0022112006008627 Published online by Cambridge University Press

The quality of the non-parallel basic flow is important because it is one of the elements that structure the perturbative equations. The sensitivity of the Orr-Sommerfeld (OS) and operator to modifications of the basic flow has recently been considered for plane Couette flow by Bottaro, Corbett & Luchini (2003) in terms of the differences between the laboratory flow and its theoretical counterpart. In the same way, it can be inferred that the differences between simplified models of Navier–Stokes near-parallel solutions (usually given in terms of the streamwise momentum distribution only) and their theoretical equivalents, which instead explicitly include lateral dynamics, will also originate variations of the OS eigenvalues.

In this context, we analyse the convective instability of a new analytical wake solution that is very accurate in the intermediate and far fields, where instability is convective. This solution (Tordella & Belan 2003; Belan & Tordella 2002) is described in § 2 and was obtained by matching inner and outer expansion solutions that both satisfy the Navier-Stokes model. The adoption of that model in the outer region also corresponds to a new analytical approach, which takes into account the fact that the nonlinear convection and the diffusion are comparable in the lateral far field, and uses matching criteria based on the vorticity, entrainment and pressure gradient matching. Note also that the analytical nature of the base solution is an advantage for the study of instability, because it makes the link between the steady equilibrium flow, the coefficients of the perturbation operator and associated amplitude equation, and the instability characteristics explicit, see § 3. In this analysis, by adopting spatio-temporal multiscaling, the equation that represents the evolution of disturbances is of the form $\partial_{t_1}\theta_1 + \tilde{p}(x_1)\partial_{x_1}\theta_1 + \varepsilon\tilde{q}(x_1)\theta_1 = 0$, where θ_1 is a phase function, x_1, t_1 are the slow space and time variables and ε is a small parameter equal to the inverse of the Reynolds number. The modulation evolution allows the first-order correction of the instability characteristics to be determined. We considered the modulation of two-dimensional periodic perturbations with a wavenumber corresponding to that of the saddle point of the zero-order local dispersion relation (parametric OS), taken at different positions downstream and Reynolds numbers. The relevant instability characteristics variations are described in § 4.

2. Non-parallel basic flow

An approximate Navier-Stokes solution for the region of the two-dimensional steady bluff body wake where the non-parallelism of the streamlines is not yet negligible is considered. This region is intermediate between the near field, which includes the two symmetrical counter-rotating eddies, and the ultimate far wake, see figure 1. Recognition of the existence of an intermediate asymptotics (Barenblatt 1996) is important, as the existence of a longitudinal intermediate region physically introduces the adoption of the thin shear layer hypothesis, and relevant near-similar variable transformations for the inner flow, while also supporting a differentiation of the behaviour of the intermediate flow with respect to its infinite asymptotics. The analytical representation here used accounts for the effects of the streamwise diffusion, nonlinear convection and entrainment at the lower orders and for the pressure gradient and linear and nonlinear exchange of vorticity from the inner toward the outer part of the flow at the higher orders (Belan & Tordella 2002; Tordella & Belan 2003). At the first order, the multiscaling allows the insertion of these lower order effects, through, perhaps for the first time, the explicit use of the transversal momentum component of the primary flow. The solution was obtained by matching an inner solution – a Navier-Stokes expansion in powers of the inverse

https://doi.org/10.1017/S0022112006008627 Published online by Cambridge University Press

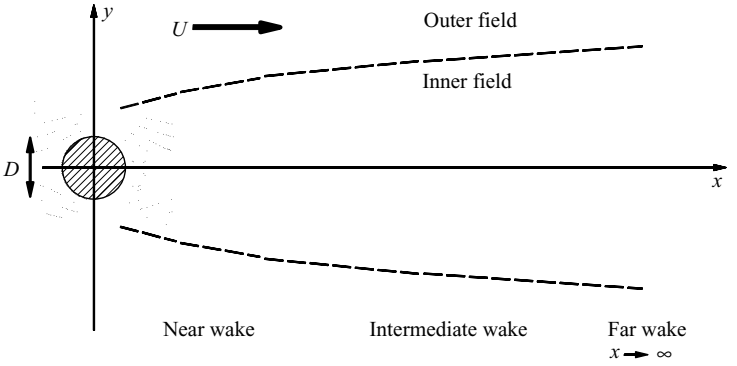


FIGURE 1. Flow schematic.

of the longitudinal coordinate ($x^{-n/2}, n = 0, 1, 2, \ldots$) – and an outer solution, which is a Navier-Stokes asymptotic expansion in powers of the inverse of the distance from the body. The matching was built on the criteria that, where the two solutions meet, the pressure longitudinal gradients and the vorticities must be equal and the flow towards the inner layer must be equal to the outflow from the external stream. The lateral decay is found to be algebraic at high orders in the inner expansion solution. Assuming the inner expansion as being an approximation of the primary wake flow and using the quasi-similar transformation

$$x = x, \ \eta = x^{-1/2} y, \tag{2.1}$$

where (x, y) are the non-dimensional longitudinal and normal coordinates, the non-dimensional velocity components (u, v), up to $O(x^{-3/2})$, can be written as

$$u = 1 + x^{-1/2}\phi_1(\eta) + x^{-1}\phi_2(\eta) + x^{-3/2}\phi_3(\eta), \tag{2.2}$$

$$v = x^{-1}\chi_1(\eta) + x^{-3/2}\chi_2(\eta). \tag{2.3}$$

The non-dimensionalization is based on the characteristic length D of the body that generates the wake, the density ρ and the velocity U of the free stream. The Reynolds number is defined as $Re = UD/\nu$, where ν is kinematic viscosity of the fluid. According to the multiscale approach, the slow spatial and temporal variables

$$x_1 = \varepsilon x, \ t_1 = \varepsilon t, \tag{2.4}$$

where $\varepsilon = 1/Re$, are introduced. Since $\eta = (Re\, x_1)^{-1/2}\, y$ the velocity components of the basic flow can also be written as

$$u = \partial_y \Psi = u_0(x_1, y) + \varepsilon u_1(x_1, y) + \cdots, \tag{2.5}$$

$$v = -\partial_x \Psi = -\varepsilon \partial_{x_1} \Psi = \varepsilon v_1(x_1, y) + \cdots. \tag{2.6}$$

By only considering the integer powers of ε, (2.2), (2.3) can assume the multiscale structure (2.5), (2.6). For the u component the result is

$$\begin{aligned} u &= 1 + Re^{-1/2}x_1^{-1/2}\phi_1(\eta) + Re^{-1}x_1^{-1}\phi_2(\eta) + Re^{-3/2}x_1^{-3/2}\phi_3(\eta) \\ &= \left[1 + Re^{-1/2}x_1^{-1/2}\phi_1(\eta)\right] + \varepsilon\left[x_1^{-1}\phi_2(\eta) + Re^{-1/2}x_1^{-3/2}\phi_3(\eta)\right], \end{aligned}$$

https://doi.org/10.1017/S0022112006008627 Published online by Cambridge University Press

so that

$$u_0 = 1 + Re^{-1/2}x_1^{-1/2}\phi_1 = 1 - x_1^{-1/2}Re^{-1/2}C_1 e^{-y^2/(4x_1)}, \tag{2.7}$$

$$\begin{aligned} u_1 &= x_1^{-1}\phi_2 + Re^{-1/2}x_1^{-3/2}\phi_3 \\ &= -x_1^{-1}\frac{C_1^2}{2}e^{-y^2/(4x_1)}\left\{C_2\,{}_1\mathrm{F}_1\left(-\frac{1}{2},\frac{1}{2};\frac{y^2}{4x_1}\right) + e^{-y^2/(4x_1)} + \sqrt{\frac{\pi}{x_1}}\frac{y}{2}\,\mathrm{erf}\left(\frac{y}{2\sqrt{x_1}}\right)\right\} \\ &\quad - x_1^{-3/2}Re^{-1/2}C_1^3(y^2/x_1 - 2)\left[\tfrac{1}{2}C_3 - Re\,F_3(y/\sqrt{Re\,x_1})\right], \end{aligned} \tag{2.8}$$

where constants C_1, C_2 and C_3 are integration constants that depend on the Reynolds number (see Belan & Tordella 2002). Function ${}_1\mathrm{F}_1$ is the confluent hypergeometric function, and F_3 is the particular case, for $n = 3$, of the general nth-order function

$$F_n(\eta) = \int_0^\eta \frac{e^{Re\,\eta'^2/4}}{\mathrm{Hr}_{n-1}^2(\eta')}\,G_n(\eta')\,\mathrm{d}\eta'; \quad G_n(\eta) = C_1^{-n}\int_0^\eta M_n(\eta')\,\mathrm{Hr}_{n-1}(\eta')\,\mathrm{d}\eta',$$

where the function $\mathrm{Hr}_{n-1}(\eta) = \mathrm{H}_{n-1}(\frac{1}{2}Re^{1/2}\eta)$ is defined in terms of the Hermite polynomials. Function $M_n(\eta)$ is the sum of the inhomogeneous terms of the general ordinary differential equation for ϕ_n, $n \geqslant 1$, obtained from the x component of the Navier–Stokes equation (see Tordella & Belan 2003). Function M_n includes the effects of the streamwise pressure gradient and diffusion terms and also of part of the longitudinal convection term.

At the same approximation order, the v component is given by

$$v = Re^{-1}x_1^{-1}\chi_1(\eta) + Re^{-3/2}x_1^{-3/2}\chi_2(\eta) = \varepsilon\left[x_1^{-1}\chi_1(\eta) + Re^{-1/2}x_1^{-3/2}\chi_2(\eta)\right] \tag{2.9}$$

so that

$$\begin{aligned} v_1 &= x_1^{-1}\chi_1 + x_1^{-3/2}Re^{-1/2}\chi_2 = \frac{1}{2}x_1^{-3/2}Re^{-1/2} \\ &\times \left\{-C_1\,y\,e^{-y^2/4x_1} + \left[\Phi_2\left(\frac{y}{\sqrt{Re\,x_1}}\right) + \frac{y}{\sqrt{Re\,x_1}}\phi_2\left(\frac{y}{\sqrt{Re\,x_1}}\right)\right]\right\} \end{aligned} \tag{2.10}$$

where ϕ_2 is the function coefficient of the u expansion at the order x^{-1}, which is also present in (2.8), and $\Phi_2 = \int \phi_2\,\mathrm{d}\eta$.

3. Multiscale analysis

The multiscale approach leads to the following hypothesis for the perturbation of the stream function:

$$\psi = \varphi(x, y, t; \varepsilon) = [\varphi_0(x_1, y, t_1) + \varepsilon\varphi_1(x_1, y, t_1) + \cdots]\,e^{i\theta_0(x,t;\varepsilon)}. \tag{3.1}$$

By rewriting $\varphi_0(x_1, y, t_1) = A(x_1, t_1)\zeta_0(x_1, y)$ and $\varphi_1(x_1, y, t_1) = A(x_1, t_1)\zeta_1(x_1, y)$, where $A(x_1, t_1) = e^{i\theta_1(x_1,t_1)}$ is a slow spatio-temporal modulation factor (Bouthier 1972), the perturbation takes the form

$$\psi = (\varphi_0 + \varepsilon\varphi_1 + \cdots)\,e^{i\theta_0} = A(\zeta_0 + \varepsilon\zeta_1 + \cdots)\,e^{i\theta_0} = (\zeta_0 + \varepsilon\zeta_1 + \cdots)\,e^{i\theta_0 + i\theta_1 + \cdots}. \tag{3.2}$$

The complete phase becomes $\theta = \theta_0 + \theta_1 + \cdots$, and according to the Whitham theory (Whitham 1974)

$$\partial_x\theta = h = (k + is), \;\; \partial_t\theta = -\sigma = -(\omega + ir), \tag{3.3}$$

https://doi.org/10.1017/S0022112006008627 Published online by Cambridge University Press

where h and σ are the complex dimensionless wavenumber and pulsation ($k = \mathrm{Re}(h)$ wavenumber, $s = \mathrm{Im}(h)$ spatial growth rate, $\omega = \mathrm{Re}(\sigma)$ circular frequency, $r = \mathrm{Im}(\sigma)$ temporal growth rate), so that $\partial_x\theta_0 = h_0 = (k_0 + \mathrm{i}s_0)$ and $\partial_t\theta_0 = -\sigma_0 = -(\omega_0 + \mathrm{i}r_0)$.

In terms of x_1, t_1 and θ_0 the spatial and temporal derivatives transform as

$$\partial_x \to h_0\partial_{\theta_0} + \varepsilon\partial_{x_1} + \cdots, \quad \partial_y \to \partial_y, \quad \partial_t \to -\sigma_0\partial_{\theta_0} + \varepsilon\partial_{t_1} + \cdots. \tag{3.4}$$

Due to the multiscaling, the complete (order 0 + order 1) wavenumber and pulsation will be $h = \partial\theta/\partial x = h_0\partial\theta/\partial\theta_0 + \varepsilon\partial\theta_1/\partial x_1 + \cdots = h_0 + \varepsilon h_1 + \cdots$ and $\sigma = -\partial\theta/\partial t = -\sigma_0\partial\theta/\partial\theta_0 + \varepsilon\partial\theta_1/\partial t_1 + \cdots = -(\sigma_0 + \varepsilon\sigma_1 + \cdots)$, where the first-order corrections of the instability characteristics will be obtained as

$$h_1 = (k_1 + \mathrm{i}s_1) = \partial\theta_1/\partial x_1, \ \sigma_1 = (\omega_1 + \mathrm{i}r_1) = -\partial\theta_1/\partial t_1. \tag{3.5}$$

According to Bouthier (1972), by applying the derivative transformations (3.4) to the linearized equations for the perturbation of the stream function, a hierarchy of ODEs are obtained. The zero-order equation is the parametric Orr-Sommerfeld equation, where x_1 and the Reynolds number Re are parameters,

$$\mathscr{A}\,\varphi_0 \;=\; \sigma_0\,\mathscr{B}\,\varphi_0, \tag{3.6}$$

with $\mathscr{A} = \{(\partial_y^2 - h_0^2)^2 - \mathrm{i}h_0 Re[u_0(\partial_y^2 - h_0^2) - u_0'']\}$, $\mathscr{B} = -\mathrm{i}Re(\partial_y^2 - h_0^2)$. The modulation A, unknown at this order, describes the transmission of the instability wave from one near-parallel region to the next and is determined at the next order. The first-order multiscaling equation is inhomogeneous:

$$\mathscr{A}\,\varphi_1 \;=\; \sigma_0\,\mathscr{B}\,\varphi_1 \;+\mathscr{M}\varphi_0. \tag{3.7}$$

The operator $\mathscr{M}$ is

$$\begin{aligned}\mathscr{M} = \big\{ &\big[Re\big(2h_0\sigma_0 - 3h_0^2u_0 - u_0''\big) + 4\mathrm{i}h_0^3\big]\partial_{x_1} + (Re\,u_0 - 4\mathrm{i}h_0)\partial^3_{x_1yy} - Re\,v_1\big(\partial_y^3 - h_0^2\partial_y\big)\\ &+ Re\,v_1''\partial_y + \mathrm{i}h_0 Re\big[u_1\big(\partial_y^2 - h_0^2\big) - u_1''\big] + Re\big(\partial_y^2 - h_0^2\big)\partial_{t_1}\big\}.\end{aligned} \tag{3.8}$$

Note that $\mathscr{M}$ is a function of the full basic flow, also of the transversal momentum v_1 and thus of the entrainment, as well as of the zero-order dispersion relation and eigenfunctions. To avoid secular terms in the solution of (3.7), a solvability condition has to be satisfied. This condition requires that the inhomogeneous term in (3.7) is orthogonal to each solution of the adjoint homogenous problem. This yields

$$\begin{aligned}&(\partial_{x_1}A)\int_{-\infty}^{\infty}\zeta_0^+\left[M_1 + M_2\partial_y^2\right]\zeta_0\,\mathrm{d}y + (\partial_{t_1}A)\int_{-\infty}^{\infty}\zeta_0^+\left[M_7 + M_8\partial_y^2\right]\zeta_0\,\mathrm{d}y\\ &\quad + A\int_{-\infty}^{\infty}\zeta_0^+\left[M_1\partial_{x_1} + M_2\partial^3_{x_1yy} + M_3 + M_4\partial_y + M_5\partial_y^2 + M_6\partial_y^3\right]\zeta_0\,\mathrm{d}y = 0.\end{aligned} \tag{3.9}$$

where the coefficients M_j are function of x_1, y:

$$\left.\begin{aligned}&M_1 = Re\big(2h_0\sigma_0 - 3h_0^2u_0 - u_0''\big) + 4\mathrm{i}h_0^3, \quad M_2 = Reu_0 - 4\mathrm{i}h_0,\\ &M_3 = -\mathrm{i}h_0 Re\big(\partial_y^2 + h_0^2\big)u_1, \quad M_4 = -Re\big(\partial_y^2 + h_0^2\big)v_1,\\ &M_5 = \mathrm{i}h_0 Reu_1, \quad M_6 = Rev_1, \quad M_7 = -Reh_0^2, \quad M_8 = Re.\end{aligned}\right\} \tag{3.10}$$

and ζ_0^+ is the perturbation stream function of the homogeneous adjoint problem. Note that, when the multiscaling is only spatial, coefficients M_7, M_8 do not exist and this leads to the simple modulation equation $\mathrm{d}_{x_1}A(x_1) = \mathrm{i}h_1(x_1)A(x_1)$, where h_1 depends on

https://doi.org/10.1017/S0022112006008627 Published online by Cambridge University Press

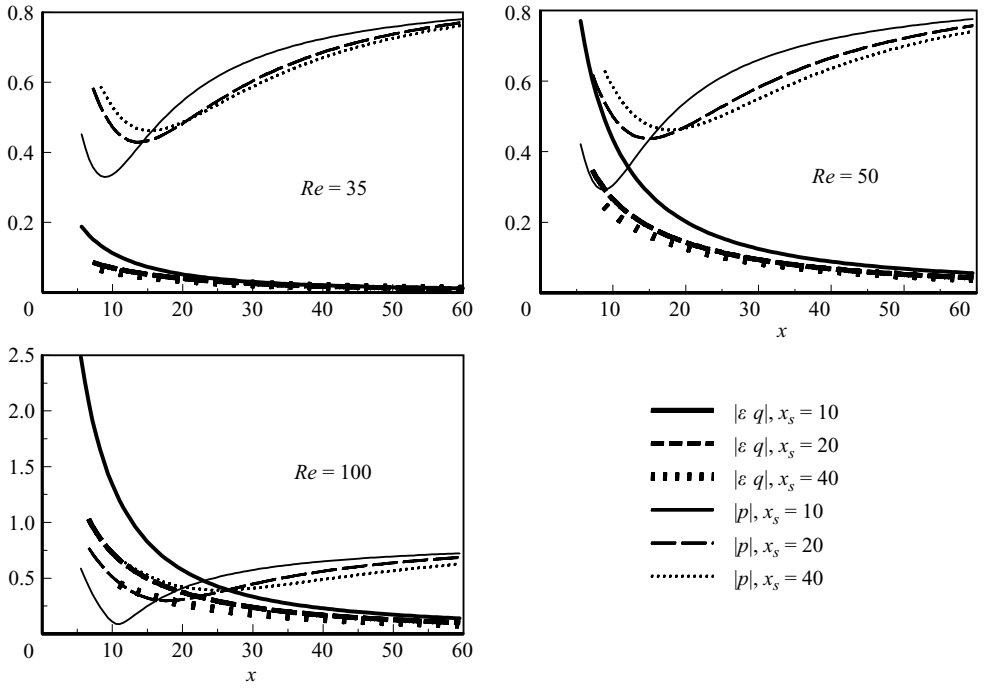


FIGURE 2. Coefficients of the modulation equation (3.11) for perturbations centred around $x_s \simeq 10, 20, 40$, with $Re = 35, 50, 100$.

the $M_i, i = 1, \ldots, 6$, see Tordella & Belan (2005). By recalling that $A(x_1, t_1) = \mathrm{e}^{\mathrm{i}\theta_1(x_1,t_1)}$, and going back to the original coordinates x, and t, (3.9) can be written as

$$\partial_t \theta_1 + p(x)\partial_x \theta_1 + \varepsilon q(x)\theta_1 = 0 \tag{3.11}$$

where coefficients

$$p(x) = \frac{\displaystyle\int_{-\infty}^{\infty} \zeta_0^+ \left[M_1 + M_2 \partial_y^2\right] \zeta_0 \, \mathrm{d}y}{\displaystyle\int_{-\infty}^{\infty} \zeta_0^+ \left[M_7 + M_8 \partial_y^2\right] \zeta_0 \, \mathrm{d}y} \tag{3.12}$$

and

$$q(x) = \frac{\displaystyle\int_{-\infty}^{\infty} \zeta_0^+ \left[M_1 \partial_{x_1} + M_2 \partial^3_{x_1 yy} + M_3 + M_4 \partial_y + M_5 \partial_y^2 + M_6 \partial_y^3\right] \zeta_0 \, \mathrm{d}y}{\displaystyle\int_{-\infty}^{\infty} \zeta_0^+ \left[M_7 + M_8 \partial_y^2\right] \zeta_0 \, \mathrm{d}y} \tag{3.13}$$

are not singular.

The disturbance and the basic flow determine the coefficients p and q. We consider the system to be disturbed by a wave with wavenumber equal to that of the less stable mode at a given position $x = x_s$, that is then parametrically varied in the domain. In such a way, the system in $x = x_s$ is tuned to the appropriate characteristics corresponding to the dominant saddle point of the local dispersion relation. We call this position $x = x_s$ the centre of the perturbation. The distribution of the module of the coefficients of the modulation equation (3.11) is shown in figure 2, for three perturbations centred around $x_s = 10.50, 20.95, 40.20$ and for $Re = 35, 50, 100$.

https://doi.org/10.1017/S0022112006008627 Published online by Cambridge University Press

Relations (3.13), and (3.12) highlight the different physical contents of the two modulation coefficients. In q are present the coefficients M_j, $j = 3 \ldots, 6$, that depend on the first-order longitudinal u_1, but also crosswise v_1, momentum distributions. This information is not in p. Only the zero-order longitudinal momentum u_0 appears in p. This explains the large difference that, at a given x, can exist between p and q. In particular, in the interval $x \in [5, 60]$ where the non-parallel corrections are computed, it can be seen that on increasing Re, from 35 to 100, εq increases by one order of magnitude near the beginning of the domain, while p remains almost unchanged in the interval of values $[0, 0.8]$, see figure 2. Thus q is very sensitive to the variation of the entrainment intensity with Re, that is, to the acquisition of lateral momentum in the wake.

The modulation equation (3.11) can be solved numerically by specifying the initial state and the boundary conditions on the domain of validity of the theory (which extends from a few body scales D downstream of the body, to the far field, $x_f \gg D$, in the present computations from $x = 5$ to $x = 60$). Having only one boundary condition available, it can be used to impose the asymptotic uniformity of the modulation in the far field:

$$(\partial_x \theta_1)_{x=x_f} = 0, \ \forall\, t. \tag{3.14}$$

With regards to the initial condition, a natural choice is

$$(\theta_1)_{(x,t=0)} = (\text{const})\,(1 + \mathrm{i}). \tag{3.15}$$

4. Streamwise distribution of the instability characteristics

By numerically solving the modulation equation (3.11) and using (3.5) the first-order correction of the instability characteristics has been computed in the intermediate and far circular cylinder wake. A large difference between the complete (order 0 + order 1) problem and the order 0 problem is shown more by the pulsation ω and the temporal growth factor r, than by the wavenumber k and the spatial growth factor s.

Typically, the correction increases the values of k and s, thus it reduces the module of the spatial amplification, as the simpler spatial multiscale analysis also shows (Tordella & Belan 2005). The correction for k is higher as it approaches the body and Re is increased, see figure 3 for the disturbance centred around $x_s = 5.5$. The correction for s is negligible throughout, regardless of the Re, except for $Re = 50$ and 100 at the beginning of the domain considered here, when the perturbation relates to sections in the earlier intermediate region, i.e. in the present computation when $x_s = 5.5$, see figure 3.

Figures 4–6 show the (order 0 + correction of order 1) ω and r distributions compared with the distributions of the zero-order problem in the wake portion observed with this asymptotic theory, $x \in [5, 60]$. A first observation concerning the growth factor r is that the correction of the first order yields absolute instability from $x = 5$ to $x \approx 9$ at $Re = 50$, and from $x = 5$ to $x \approx 15$ at $Re = 100$, when the perturbation relates to sections in the early intermediate region, see figure 4. On placing x_s in $x = 10.5$, the behaviour is similar, but the absolute instability – in the portion of the wake we can see with this asymptotic theory – is reached only for $Re = 100$, see figure 4. In general, r is higher close to the body, as it decreases downstream. However, when the perturbation relates to sections in the late intermediate region, $x_s \approx 40$, no regions of absolute instability are present, and contrary to k, s, and ω the growth factor r can exhibit maximum points, i.e. points where the temporal stability

https://doi.org/10.1017/S0022112006008627 Published online by Cambridge University Press

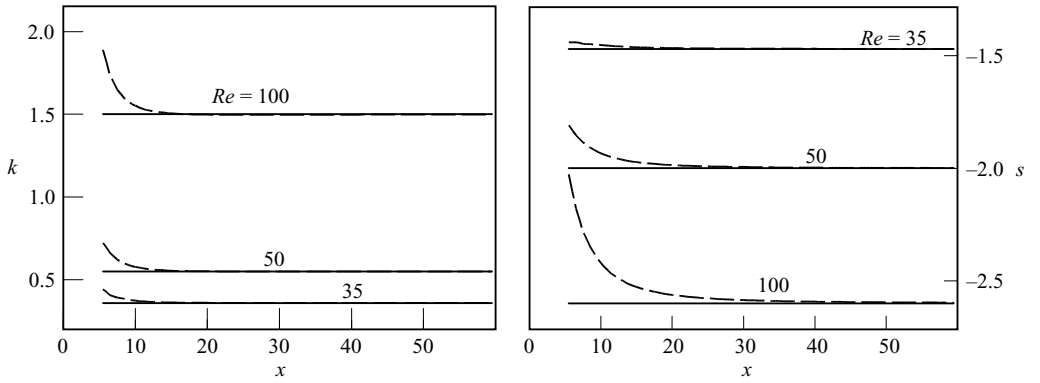


FIGURE 3. Order 0 (———) and order 0 + 1 (– – – –) wavenumber and spatial amplification factor distributions for $Re = 35, 50, 100$. The disturbance has a complex wavenumber equal to that of the dominant saddle of the local dispersion relation at $x = 5.5$, that is for $Re = 35$, $h_0 = 0.318 - 1.433\,\mathrm{i}$; for $Re = 50$, $h_0 = 0.451 - 1.913\,\mathrm{i}$; and for $Re = 100$, $h_0 = 1.030 - 2.578\,\mathrm{i}$.

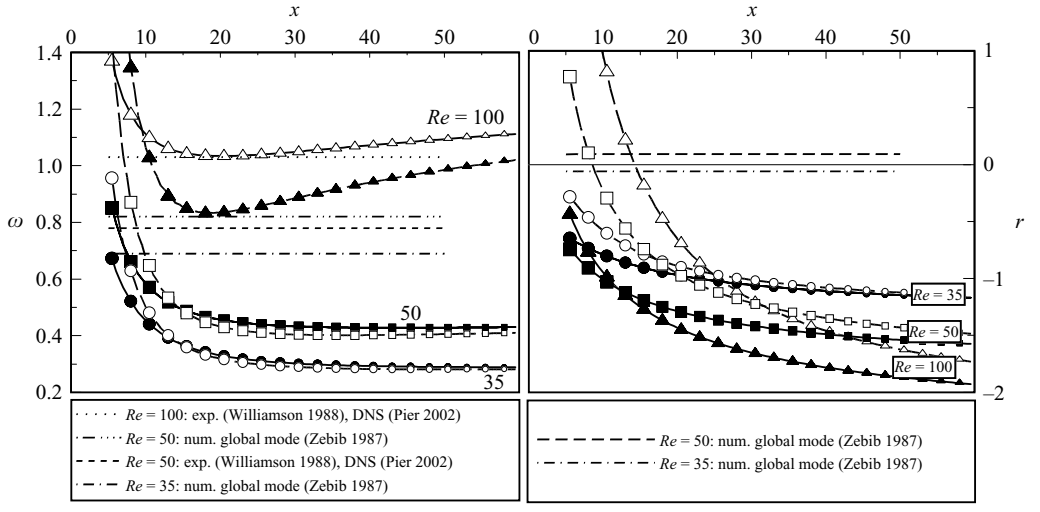


FIGURE 4. Order 0 (—, solid symbols) and order 0 + 1 (– –, open symbols) pulsation and temporal amplification factor x distributions for $Re = 35, 50, 100$. Disturbances as in figure 3. Comparison with experimental and numerical simulations results.

is minimum, see figure 6. In the far field, while the spatial amplification rate rises with Re, see figure 3, r drops out more rapidly at higher Re, see figures 4–6.

The frequency grows with Re for fixed x_s, and, fixing Re, generally decreases with x. However, a slightly different behaviour is observed for $Re = 100$ when $x_s = 5.5$. In this case, the pulsation decreases downstream, where it reaches a minimum, and then increases, settling near a pulsation value of the order of that measured in Williamson's (1988) laboratory experiment and in Pier's (2002) DNS. Examples of streamwise evolution of the complex frequency in a wide portion of the intermediate wake are rare in the literature. Pier (2002) has obtained this evolution up to $x = 20$ ignoring flow non-parallelism and deriving the local characteristics by freezing the x-coordinate and studying the equivalent parallel shear flow. Figure 2 in Pier (2002), shows that the x trend of the frequency and temporal growth factor is qualitatively

https://doi.org/10.1017/S0022112006008627 Published online by Cambridge University Press

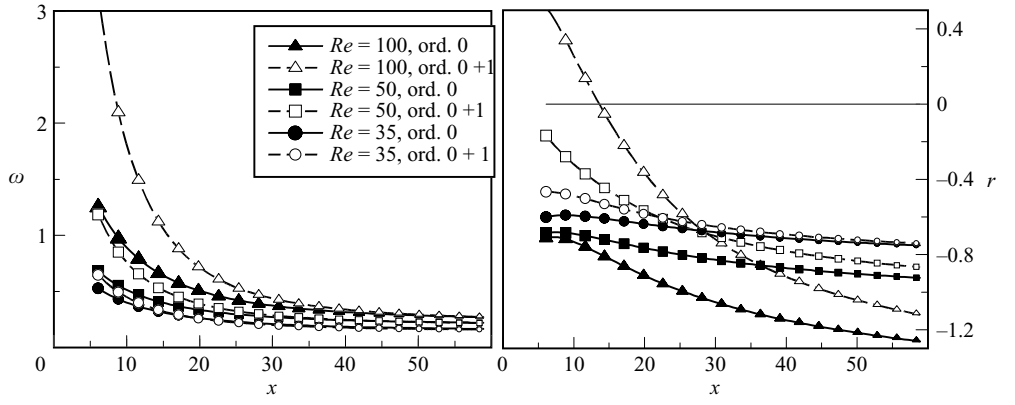


FIGURE 5. As figure 4 but with complex wavenumber equal to that of the dominant saddle of the local dispersion relation at $x = 10.5$, that is for $Re = 35$, $h_0 = 0.17 - 0.95\,\mathrm{i}$; for $Re = 50$, $h_0 = 0.24 - 1.17\,\mathrm{i}$; and for $Re = 100$, $h_0 = 0.28 - 1.76\,\mathrm{i}$.

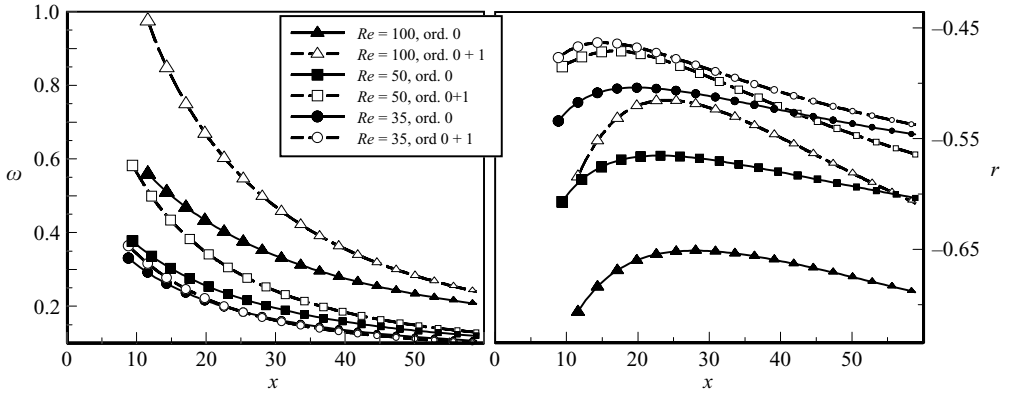


FIGURE 6. As figure 4 but with complex wavenumber equal to that of the dominant saddle of the local dispersion relation at $x = 40.2$, that is for $Re = 35$, $h_0 = 0.078 - 0.69\,\mathrm{i}$; for $Re = 50$, $h_0 = 0.074 - 0.77\,\mathrm{i}$; and for $Re = 100$, $h_0 = 0.10 - 0.95\,\mathrm{i}$.

analogous, under similar conditions, to the trend obtained here. Note that we are *a priori* excluding the near wake from our analysis, consistently with the hypothesis that we have adopted for the asymptotic expansion of the basic flow. Data from the global results obtained by Pier (2002, DNS simulations), Williamson (1988, laboratory observations) and Zebib (1987, numerical experiments) are included in figure 4. The values of the global pulsation obtained in these numerical and laboratory experiments are in good agreement with the complex frequency obtained in this study in the first part of the intermediate wake.

5. Conclusions

An analytical representation of the base flow which also accurately describes the cross-stream momentum evolution has been used in this work. First-order spatio-temporal multiscaling yields a complex modulation equation that contains the information on the dynamics of the flow in the coefficients. In particular, the lateral momentum evolution and the entrainment process are included. As a consequence,

https://doi.org/10.1017/S0022112006008627 Published online by Cambridge University Press

the correction of the instability characteristics downstream to the body is obtained in a way that takes these aspects into account.

An enriched description of the convective instability is obtained where the wavenumber and the complex frequency vary rapidly at the beginning of the intermediate wake. Variations increase with Re. For $Re = 50$ and 100, extended regions of absolute instability are reached when the disturbance has a wavenumber equal to that of the saddle point of the dispersion relation of a section located in the early part of the intermediate wake. When the disturbance relates to sections of the late intermediate wake the temporal growth factor r has points of minimal temporal stability. In the far field, r falls more rapidly at higher Re. The global values found in laboratory and DNS experiments are close to the complex frequency obtained in the first part of the intermediate wake when the disturbances relate to these sections.

The authors would like to thank Professor W. O. Criminale for many helpful discussions, critical reading and interest in the progress of the work.

REFERENCES

Barenblatt, G. I. 1996 *Scaling, Self-similarity, and Intermediate Asymptotics*, Cambridge University Press, Preface, p. xiii.

Belan, M. & Tordella, D. 2002 Asymptotic expansions for two-dimensional symmetrical laminar wakes. *Z. Angew. Math. Mech.* **82**, 219–234.

Bottaro, A., Corbett, P. & Luchini, P. 2003 The effect of base flow variation on flow stability. *J. Fluid Mech.* **476**, 293–302.

Bouthier, M. 1972 Stabilité linéare des écoulements presque parallèles. *J. Mec.* **11**, 599–621.

Chomaz, J. M., Huerre, P. & Redekopp, L. G. 1991 A frequency selection criterion in spatially developing flows. *Stud. Appl. Maths* **84**, 119–144.

Hannemann, K. & Oertel, H. 1989 Numerical simulation of the absolutely and convectively unstable wake. *J. Fluid Mech.* **199**, 55–88.

Mattingly, G. E. Jr & Criminale, W. O. 1972 The stability of an incompressible two-dimensional wake. *J. Fluid Mech.* **51**, 233–276.

Monkewitz, P. A. 1988 The absolute and convective nature of instability in two-dimensional wakes at low Reynolds numbers. *Phys. Fluids* **31**, 999–1006.

Monkewitz, P. A., Huerre, P. & Chomaz, J. M. 1993 Global linear-stability analysis of weakly nonparallel shear flows. *J. Fluid Mech.* **251**, 1–20.

Pier, B. 2002 On the frequency selection of finite-amplitude vortex shedding in the cylinder wake. *J. Fluid Mech.* **458**, 407–417.

Tordella, D. & Belan, M. 2003 A new matched asymptotic expansion for the intermediate and far flow behind a finite body. *Phys. Fluids* **15**, 1897–1906.

Tordella, D. & Belan, M. 2005 On the domain of validity of the near-parallel combined stability analysis for the 2D intermediate and far bluff body wake. *Z. Angew. Math. Mech.* **85**, 51–65.

Triantafyllou, G. S., Kupfer, K. & Bers, A. 1987 Absolute Instabilities and self-sustained oscillations in the wakes of circular cylinders. *Phys. Rev. Lett.* **15**, 1897–1906.

Whitham, G. B. 1974 *Linear and Nonlinear Waves*. John Wiley & Sons.

Williamson, C. 1988 Defining a universal and continuous Strouhal-Reynolds number relationship for the laminar vortex shedding of a circular cylinder. *Phys. Fluids* **13**, 2742–2744.

Yang, X. & Zebib, A. 1989 Absolute and convective instability of a cylinder wake. *Phys. Fluids* A **1**, 689–696.

Zebib, A. 1987 Stability of viscous flow past a circular cylinder. *J. Engng Maths* **21**, 155–165.

https://doi.org/10.1017/S0022112006008627 Published online by Cambridge University Press